Kobe University Repository : Kernel

PDF issue: 2025-12-04

Fe-Assisted Hydrothermal Liquefaction of Lignocellulosic Biomass for Producing High-Grade Bio-Oil

Miyata, Yoshinori ; Sagata, Kunimasa ; Hirose, Mina ; Yamazaki, Yoshiko ; Nishimura, Aki ; Okuda, Norimasa ; Arita, Yoshitaka ; Hirano,…

(Citation)
ACS Sustainable Chemistry and Engineering,5(4):3562-3569

(Issue Date)
2017-04

(Resource Type)
journal article

(Version)
Version of Record

(Rights)
©2017 American Chemical Society. This is an open access article published under an ACS AuthorChoice License, which permits copying and redistribution of the article or any adaptations for non-commercial purposes.

(URL)
https://hdl.handle.net/20.500.14094/90004160

This is an open access article published under an ACS AuthorChoice License, which permits copying and redistribution of the article or any adaptations for non-commercial purposes.

ACS Sustainable Chemistry & Engineering

Research Article

pubs.acs.org/journal/ascecg

Fe-Assisted Hydrothermal Liquefaction of Lignocellulosic Biomass for Producing High-Grade Bio-Oil

Yoshinori Miyata,[†] Kunimasa Sagata,[‡] Mina Hirose,[‡] Yoshiko Yamazaki,[‡] Aki Nishimura,[†] Norimasa Okuda,[†] Yoshitaka Arita,[†] Yoshiaki Hirano,[‡] and Yuichi Kita*[,‡]

[†]Strategic Technology Research Center, Nippon Shokubai Co., Ltd., Suita, Osaka 564-8512, Japan

[‡]Department of Chemical Science and Engineering, Graduate School of Engineering, Kobe University, Kobe 657-8501, Japan

Supporting Information

ABSTRACT: Although bio-oils produced by pyrolysis and hydrothermal synthesis demonstrate potential toward building a sustainable society, large amounts of char generated as a byproduct and their thermal instability owing to high oxygen content hinder their applications. Hence, a novel approach for the production of high-grade bio-oil was proposed herein. In this approach, zerovalent Fe was used as an agent for generating hydrogen in situ in the hydrothermal liquefaction of oil palm empty fruit bunch (EFB), a lignocellulosic biomass source, affording bio-oil containing water-soluble (WS) and water-insoluble (WI) fractions in high yields. Hydrogen generated by the reaction between Fe and H_2O efficiently converted unstable intermediates obtained from the degradation of EFB into stable compounds, resulting in reduced char formation. Hydroxyketones were detected as components characteristic of the WS fraction in the H_2O/EFB/Fe system, which were stable under hydrothermal condition. WS fractions were treated with the HZSM-5 zeolite, affording light olefins (C_2−C_4), as well as benzene, toluene, and xylene. This conversion was more efficient with the WS fraction obtained in the presence of Fe. The liquefaction of EFB and the conversion of WS fractions into olefins via catalytic cracking were also achieved using recycled Fe.

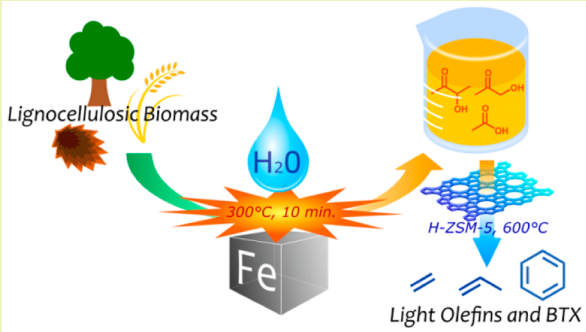

KEYWORDS: *Metallic iron, Lignocellulose, Liquefaction, Hydrogenation, Bio-oil, Hydroxyketones, Catalytic cracking, Light olefins*

INTRODUCTION

Growing concerns over the environmental impact of fossil fuels and their inevitable depletion, as well as climate change caused by greenhouse gas emissions, have led to extensive research on the development of alternative energy sources. In this regard, biomass as a possible renewable resource for energy fuels and chemicals has received significant attention.[1−3] Various researchers have investigated biomass-to-liquid (BTL) conversion as a possible method for utilizing biomass.[4]

Bio-oil produced by thermochemical processes, such as pyrolysis or hydrothermal liquefaction of biomass, is being investigated widely. It can be upgraded to transportation fuels and industrial chemicals.[5−11] Hydrothermal liquefaction, in which biomass is decomposed under subcritical or supercritical water, is a promising candidate for producing bio-oil.[7−11] Contrary to pyrolysis, hydrothermal liquefaction has the advantage of not requiring predrying the biomass feedstock, which originally contains water.[3,6] Several groups have made significant efforts to enhance the yield of liquid products in this process and suppress the formation of char.[8,10,11]

However, compared to fossil oil, bio-oil contains significantly higher amounts of water and oxygen. Hence, in terms of fuel property, it exhibits a low calorific value.[12] Because of the presence of oxygen-rich compounds, bio-oil is both chemically and thermally unstable, which hinders its direct application in the current infrastructure of oil refinery. Hence, the high oxygen content must be reduced by upgrading technologies such as hydrotreating and catalytic cracking.[13−15] Huber et al. have reported an integrated catalytic approach combining hydroprocessing with zeolite catalysis for the conversion of bio-oils into light olefins (C_2−C_4 olefins), as well as benzenes, toluene, and xylenes (BTX), which are industrial commodity chemical feedstock.[15] The upgraded bio-oil after two-step hydrogenation exhibited higher selectivity of light olefins and BTX than the crude oil. For the hydrogenation process, the cost of hydrogen would be a key factor of the economic efficiency for utilizing bio-oil as a chemical feedstock. Although renewable production of hydrogen has been developed, its cost is still high, mainly due to the high capital investment and delivery cost.[16−20]

In this context, we developed a method to produce high-quality oil directly from biomass, without requiring the necessary expensive equipment. We investigated the effect of metal Fe on the hydrothermal reaction of biomass to afford high-quality bio-oil, which involves the generation of hydrogen

Received: February 7, 2017
Published: February 27, 2017

 © 2017 American Chemical Society

DOI: 10.1021/acssuschemeng.7b00381
ACS Sustainable Chem. Eng. 2017, 5, 3562−3569

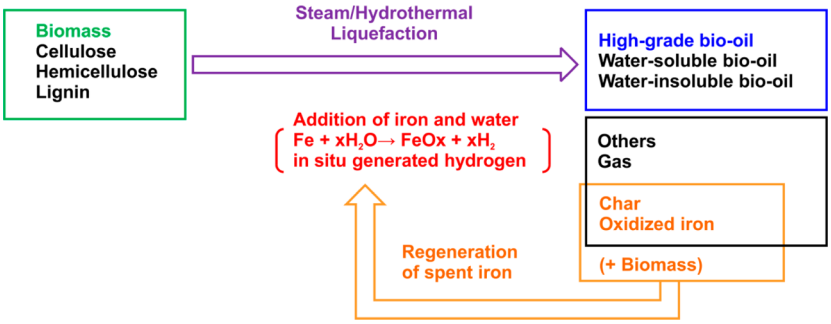

Figure 1. Overview of the liquefaction of biomass using hydrogen generated in situ from Fe and H_2O.

in situ from the reaction between metal and water. This system promotes the decomposition of biomass while simultaneously performing hydrogenation (shown in Figure 1). Char by-product produced during the reaction can be used as a reductant for regenerating the oxidized metal. Therefore, this process as a whole is carbon neutral and environmentally friendly. We report the reactivity of oil palm empty fruit bunch (EFB) in hydrothermal liquefaction, the effect of Fe as the hydrogen-generating agent, and the regeneration of oxidized Fe. In addition, we show the conversion of the water-soluble fraction into C_2−C_4 olefins and aromatics over an HZSM-5 zeolite catalyst.

■ EXPERIMENTAL SECTION

Materials. Oil palm empty fruit bunch (EFB) from Indonesia was supplied from Nippon Shokubai Co., Ltd. (Japan), and it was used as the lignocellulosic biomass feedstock. EFB was dried at 25 °C and crushed into particles with a size of less than 300 μm. Table S1 shows the EFB composition.[21] Moisture and ash content were determined by thermogravimetry at 120 and 1000 °C (EXSTAR TG/DTA 7200, Hitachi High-Tech Science Corporation). Fe powder (99.9%, NM-0029-UP) was purchased from Ionic Liquids Technologies GmbH (Germany). HZSM-5 zeolite with a Si/Al ratio of 24:1 was supplied by Nippon Shokubai Co., Ltd. (Japan). All other chemicals were commercially obtained: cellulose (Avicel PH-101, Sigma-Aldrich), xylan from corn core (Tokyo Chemical Industry Co., Ltd.), D-(+)-glucose (100%, Wako Pure Chemical Industries, Ltd.), D-(+)-xylose (99.7%, Wako Pure Chemical Industries, Ltd.), dihydroxyacetone dimer (99.8%, Wako Pure Chemical Industries, Ltd.), pyruvaldehyde solution (38.4%, Wako Pure Chemical Industries, Ltd.), hydroxyacetone (99.2%, Wako Pure Chemical Industries, Ltd.), and copper powder (99.9%, Ionic Liquids Technologies GmbH).

Fe was oxidized by the following procedure. First, Fe powder (3.5 g) and H_2O (2.238 g) were introduced into a 100 mL Hastelloy C high-pressure reactor (OM Lab-Tech., MMJ-100), and the reactor was purged four times with nitrogen. Second, the reactor was heated to 300 °C, and this temperature was maintained for 10 min. Finally, after cooling the reactor to 25 °C, the oxidized Fe samples were separated by filtration, followed by drying overnight under vacuum at 70 °C.

Liquefaction and Separation. All EFB liquefaction experiments were conducted in the batch mode using the Hastelloy C high-pressure reactor. First, EFB (1.0 g), Fe powder (0 or 1.564 g), and H_2O (0, 1, 3, 5, 10, or 40 g) were introduced into the reactor, which was purged four times with nitrogen. Second, the initial pressure was set to 1.0 MPa with nitrogen, and the stirring rate was adjusted to 700 rpm. Next, the reactor was heated to 300 °C and maintained constant at that temperature for 10 min. Upon reaction completion, the reactor was rapidly cooled to 25 °C using ice water.

Bio-oil, gas, and char products were separated following a previously published method.[22] The gaseous products were collected in a gas sampling bag, and the water-soluble products were filtered and designated as "WS". Then, the reactor wall was washed with acetone, and the resulting acetone solution with the residue was filtered. The residue was rinsed with acetone repeatedly until the eluent became colorless. The final acetone solution was evaporated at 30 °C under reduced pressure, and the temperature was increased to 60 °C to remove water. The resulting residues were designated as "water-insoluble" fractions (WI). In addition, the residue from the filter paper was dried overnight at 70 °C under reduced pressure, affording the solid residue (SR).

Catalytic Cracking of Bio-Oil. A fixed-bed continuous flow reactor was utilized for the production of light olefins from WS by catalytic cracking. This reaction system consisted of a stainless steel tube reactor, gas feeding system, liquid feeding pump, heating system, gas wash bottle with ice-cold water, and gas sampling system (Figure S1). HZSM-5 zeolite (0.85−1.7 mm, 6 mL) was added into the reactor, followed by adding stainless steel beads for vaporizing the liquid feedstock. The catalyst was flushed with nitrogen (50 mL/min) for 1 h at 25 °C, followed by heating to 600 °C under nitrogen (50 mL/min). The aqueous WS solution was fed into the reactor using a plunger pump at a w8 hly space velocity of 1.1 h^{-1}. During the reaction, the condensed products were collected using the gas wash bottle with either water or acetone. All gaseous products were collected in a gas sampling bottle. Finally, the HZSM-5 catalyst was removed and crushed in a mortar for coke analysis.

Product Analysis. The organic carbon content of WS was measured using a total organic carbon analyzer (Shimadzu, TOC-$L_{CSH/CSN}$). The WS solution was analyzed by high-performance liquid chromatography (Shimadzu, Prominence) using Aminex HPX-87P and HPX-87H columns (Bio-Rad, 300 mm × 7.8 mm ID) equipped with a refractive index detector. In addition, the sample was diluted with acetone (1:1 by volume) and analyzed with a gas chromatography system (Shimadzu, GC-2010) using a capillary column (Restek, Stabilwax, 30 m × 0.25 mm ID × 0.25 μm film thickness) and a flame ionization detector. The gas chromatography−mass spectrometry (GC−MS) analysis was performed using a Shimadzu QP-2010 system equipped with a capillary column (GL Sciences, Inert-cap WAX-HT, 30 m × 0.25 mm ID × 0.25 μm film thickness). Elemental analysis (CHN) of the EFB, WI, and SR samples was performed using an elemental analyzer (Elementar Vario EL cube) using sulfanilamide as the calibration standard. The oxygen mass content was calculated by the difference. The yields of hydrothermal liquefaction and catalytic cracking were calculated as follows:

$$\text{yield of hydrothermal liquefaction (\%)} = \frac{\text{moles of carbon in product}}{\text{moles of carbon in raw material}} \times 100 \quad (1)$$

$$\text{yield of catalytic cracking (\%)} = \frac{\text{moles of carbon in product}}{\text{moles of carbon in WS fraction fed in}} \times 100 \quad (2)$$

Quantitative ^{13}C NMR spectra of the WS and WI samples were recorded on a Varian VNMRS 600 MHz spectrometer using an inverse-gated decoupling pulse sequence, a pulse angle of 90°, and a relaxation delay of 8 s.[23] Dimethyl sulfoxide (DMSO)-d_6 was used as

DOI: 10.1021/acssuschemeng.7b00381
ACS Sustainable Chem. Eng. 2017, 5, 3562−3569

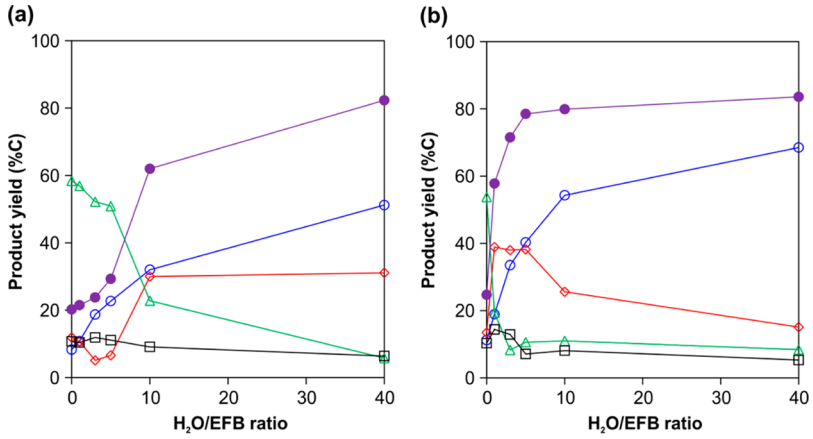

Figure 2. Yields of carbon products obtained from the liquefaction of EFB as a function of the H_2O/EFB weight ratio in the (a) absence and (b) presence of Fe. (●) WS + WI, (○) WS, (◊) WI, (□) gas, and (Δ) SR. Reaction conditions: EFB = 1.0 g, Fe = 1.564 g, H_2O = 0−40 g, P_{N2} = 1.0 MPa, temperature = 300 °C, time = 10 min.

the solvent. The molar distribution of carbon in the WS and WI fractions was determined as follows:

$$\text{molar distribution of carbon (\%)} = Y_{\text{WS or WI}} \times \frac{A_{\text{each chemical shift region}}}{A_{\text{all chemical shift regions}}} \quad (3)$$

Here, $Y_{\text{WS or WI}}$ represents the carbon yield of the WS or WI fraction, $A_{\text{each chemical shift region}}$ represents the total peak area of each chemical shift, and $A_{\text{all chemical shift regions}}$ represents the total peak area of all chemical shifts (0−230 ppm). Gaseous products were analyzed using two gas chromatography systems: Shimadzu GC-8A equipped with silica gel (Shinwa Chemical Industries, ZS-74) and molecular sieve 5A (Shinwa Chemical Industries, ZM-1) columns with a thermal conductivity detector for CO_2 and CO, and Shimadzu GC-2014 equipped with a Sunpak-A column (Shinwa Chemical Industries, ZS-72) with a flame ionization detector for hydrocarbons.

Regeneration of Fe. The fixed-bed continuous flow reactor was utilized for the regeneration of the used Fe sample, i.e., reduction of oxidized Fe. First, char-containing oxidized Fe (3.85 g) was mixed with EFB (1.93 g) using a mortar for 10 min. Second, the resulting mixture was added into a quartz reactor and heated to 1000 °C at a heating rate of 10 °C/min under nitrogen (100 mL/min), and the final temperature was maintained for 2 h. Third, the reactor was cooled to 25 °C, and the resulting Fe sample was reused for the liquefaction of EFB. The crystalline phase of the regenerated sample was determined using a Rigaku SmartLab diffractometer with CuKα radiation. Finally, in situ high-temperature X-ray diffraction (HT-XRD) measurements of the oxidized Fe and EFB mixture were performed on a Rigaku RINT TTR3 diffractometer under nitrogen (500 mL/min) using Cu Kα radiation.

RESULTS AND DISCUSSION

Effect of H_2O/EFB Weight Ratio on the Liquefaction of EFB in the Absence or Presence of Fe. The hydrothermal liquefaction of EFB with and without Fe was performed at varying H_2O/EFB weight ratios between 0:1 and 40:1. The amount of saturated water vapor in the reaction system at 300 °C was ∼3.5 g. As such, all H_2O existed as steam at H_2O/EFB ≤ 3:1, whereas a portion of the H_2O also existed in the condensed phase at H_2O/EFB ≥ 5:1. Figure 2 shows the effect of water content on the hydrothermal liquefaction of EFB. As shown in Figure 2a, in the absence of Fe, the yield of bio-oil (WS + WI) gradually increased from 20% to 29% with increasing H_2O/EFB ratio from 0:1 to 5:1; at a H_2O/EFB ratio of 40:1, the yield of bio-oil further increased to 82%. On the other hand, with increasing H_2O/EFB ratio, the SR yield consistently decreased. As shown in Figure 2b, in the presence of Fe, the yield of bio-oil drastically increased from 25% to 79% with increasing H_2O/EFB ratio from 0:1 to 5:1, whereas the yield of SR decreased. At a H_2O/EFB ratio of 40:1, the corresponding yield of bio-oil increased to 84%. Thus, although the yield of bio-oil increased with the H_2O/EFB ratio both in the presence and absence of Fe, Fe exhibits a more pronounced effect at low H_2O/EFB ratios. As the solvent can dilute the degradation products and suppress polymerization,[24,25] the increase in the yield of bio-oil with increasing H_2O/EFB ratio is tentatively attributed to the inhibition of repolymerization and the formation of carbonized products by dilution with H_2O. Similar yields for CO and CO_2 (∼10%) were observed for all systems.

Promotion of EFB Liquefaction by Fe. *H_2O/EFB Weight Ratio = 1:1.* As discussed above, the yield of bio-oil from the liquefaction of EFB was enhanced by Fe at any given H_2O content. The generation of hydrogen from the reaction between Fe and H_2O ($3Fe + 4H_2O \rightarrow Fe_3O_4 + 4H_2$) is a key reaction in the H_2O/EFB/Fe system. As summarized in Table S2, H_2 was both produced and consumed during the liquefaction of EFB.

To confirm the effect of H_2 produced from Fe and H_2O, control experiments were conducted at a H_2O/EFB ratio of 1:1, as summarized in Table 1. In the presence of oxidized Fe or Cu,

Table 1. Effect of the Addition of Fe on the Liquefaction of EFB at a H_2O/EFB Weight Ratio = 1:1[a]

Reaction system	Atmosphere	Carbon yield (%C)				Carbon balance (%)
		WS	WI	Gas	SR	
H_2O/EFB	N_2	11	11	10	57	89
H_2O/EFB/Fe[b]	N_2	19	39	14	19	91
H_2O/EFB/ Oxidized Fe[c]	N_2	13	18	12	49	92
H_2O/EFB/Cu[d]	N_2	11	11	11	55	88
H_2O/EFB	$N_2 + H_2$[e]	12	16	7	53	88

[a]Reaction conditions: EFB = 1 g, H_2O = 1 g, P_{N2} = 1.0 MPa, temperature = 300 °C, time = 10 min. [b]Fe = 1.564 g. [c]Oxidized Fe = 2.161 g. Oxidized Fe was prepared by the treatment of Fe powder with H_2O at 300 °C for 10 min (see Experimental Section). [d]Cu = 1.779 g. [e]1.0 MPa N_2 + 1.0 MPa H_2.

DOI: 10.1021/acssuschemeng.7b00381
ACS Sustainable Chem. Eng. 2017, 5, 3562−3569

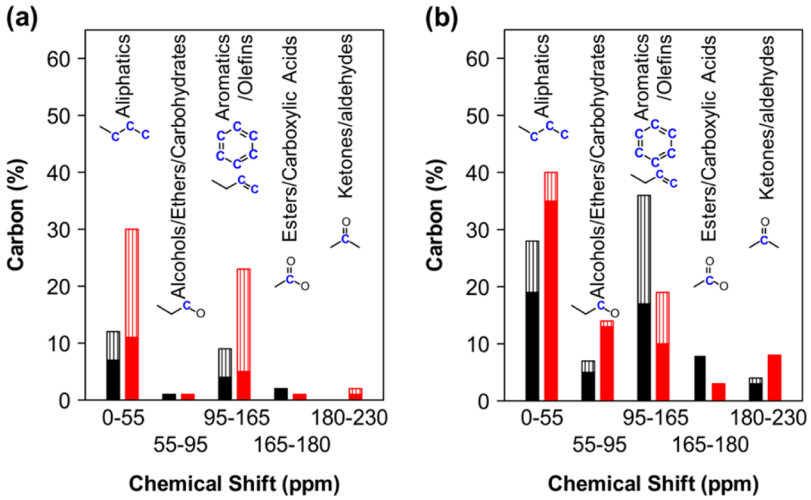

Figure 3. ^{13}C NMR spectral distribution of functional groups in the bio-oil obtained at H_2O/EFB weight ratios of (a) 1:1 and (b) 40:1, and in the absence (black bar) or presence (red bar) of Fe (Plain:WS/Striped:WI).

both of which produce no hydrogen, only marginal variation was observed with respect to the yield of bio-oil. Cu exhibits high thermal conductivity, however it did not affect the yield of bio-oil. Thus, the increased yield of bio-oil in the presence of Fe is not due to the thermal conductivity of Fe. Furthermore, the H_2O/EFB system had similar yield of bio-oil with or without 1 MPa of added H_2 gas. These results indicate that hydrogen generated from Fe and H_2O in situ apparently is responsible for the increased of bio-oil yields.

Figure 3 shows the molar distribution of carbon in the WS and WI fractions as determined by their ^{13}C NMR spectra. The presence of aliphatic carbon (0−55 ppm); alcohols, ethers, and carbohydrates moieties (55−95 ppm); aromatics and olefins (95−165 ppm); esters and carboxylic acids (165−180 ppm); and ketones and aldehydes (180−215 ppm) was confirmed. With a H_2O/EFB ratio of 1:1 (Figure 3a), the main carbon signals were attributed to aliphatics, aromatics, and olefins, with the appearance of a few oxygenated carbon resonances. The addition of Fe resulted in the significant increase of aliphatics, aromatics, and olefins, suggesting that it increases the yield of bio-oil without increasing the oxygen content.

Fe and H_2O promote the degradation of polymeric chain of the biomass components (cellulose, hemicellulose, and/or lignin), which serve as precursors for the liquid products. Hydrogen inhibits the condensation, cyclization, and repolymerization of the intermediates and liquid products, which in turn results in reduced char formation.[8] From the above results, the increased bio-oil yield with Fe is therefore attributed to the stabilization of the EFB degradation products by the hydrogen generated in situ, resulting in reduced char formation.

H_2O/EFB Weight Ratio = 40:1. In addition, the effect of Fe addition was investigated at a H_2O/EFB weight ratio of 40:1, which resulted in the more selective production of the WS fraction, albeit with a relatively constant yield of bio-oil (WS + WI). As shown in Table 2, the distribution of products in both the H_2O/EFB and H_2O/EFB/Oxidized Fe systems was similar regardless of the presence of hydrogen gas, indicating that in this case the hydrogen generated by reacting Fe and H_2O results in the selective production of the WS fraction. From the ^{13}C NMR results shown in Figure 3b, as compared with those from the H_2O/EFB system, the liquefied products obtained from the H_2O/EFB/Fe system mainly consisted of aliphatics,

Table 2. Effect of the Addition of Fe on the Liquefaction of EFB with a H_2O/EFB Weight Ratio = 40:1[a]

		Carbon yield (%C)						
		WS						
Reaction system	Atmosphere	WS	HA[e]	HB[f]	WI	Gas	SR	Carbon balance (%)
H_2O/EFB	N_2	51	5		31	6	6	94
H_2O/EFB/Fe[b]	N_2	69	20	7	15	5	8	97
H_2O/EFB/Oxidized Fe[c]	N_2	53	5	1	29	7	8	97
H_2O/EFB	N_2+H_2[d]	57	5		35	8	6	106
H_2O/EFB/Fe[b]	N_2+H_2[d]	67	19	7	19	4	9	99
H_2O/EFB/Oxidized Fe[c]	N_2+H_2[d]	55	3	2	30	9	5	99

[a]Reaction conditions: EFB = 1 g, H_2O = 40 g, P_{N2} = 1.0 MPa, temperature = 300 °C, time = 10 min. [b]Fe = 1.564 g. [c]Oxidized Fe = 2.161 g. Oxidized Fe was prepared by the treatment of Fe powder with H_2O at 300 °C for 10 min (see Experimental Section). [d]1.0 MPa N_2 + 1.0 MPa H_2. [e]Hydroxyacetone. [f]3-hydroxy-2-butanone.

albeit with a higher amount of oxygenated functional groups and a lower amount of aromatic compounds. Interestingly, the addition of Fe suppressed the formation of carboxylic compounds, indicating that formyl groups of degraded compounds are converted into alcohols instead of carboxylic acids. These results indicate that the increased yield of WS by the addition of Fe is attributed to the suppression of the aromatization of degraded compounds, and the retention of aliphatic compounds bearing oxygen-containing functional groups.

The WS fractions obtained both in the presence and absence of Fe were characterized by GC−MS, as summarized in Table 3 (chromatograms are shown in Figure S2). Both systems were predominantly composed of acids, ketones, acyclic and cyclic aliphatic compounds, alcohols, aldehydes, esters, and aromatic compounds. Nevertheless, in both cases, small peak areas were observed for aromatic and olefinic compounds, suggesting that a majority of aromatic and olefinic compounds are present as

DOI: 10.1021/acssuschemeng.7b00381
ACS Sustainable Chem. Eng. 2017, 5, 3562−3569

Table 3. GC−MS Analysis of the WS Fraction Obtained at a H_2O/EFB Weight Ratio = 40:1 Both in the Presence and Absence of Fe

	RT (min)	Compound	Area % No Fe	Area % Fe	Group[a]		RT (min)	Compound	Area % No Fe	Area % Fe	Group[a]
1	7.22	Cyclopentanone	0.3	0.8	A-2	20	12.52	Propanoic acid	2.0	0.8	A-3
2	8.96	3-Hydroxy-2-butanone	3.2	8.1	A-1,2	21	12.66	Methyl 3-methyl-2-oxopentanoate	0.1	0.9	A-2,4
3	9.22	Hydroxyacetone	11.5	17.6	A-1,2	22	12.87	2-Methylpropanoic acid	1.2	0.3	A-3
4	9.59	3-Methyl-2-cyclopentene-1-one	0	0.3	A-2	23	13.37	2-Hydroxycyclohexanone	0	1.1	A-1,2
5	9.80	1,2-Butanediol	0.8	6.7	A-1	24	13.58	Ethylene glycol	3.8	1.7	A-1
6	9.99	4-Heptanone	1.7	5.2	A-2	25	13.62	4-Methyl-4-hexene-3-one	0	0.8	A-2
7	10.03	2-Hydroxy-3-pentanone	1.2	6.2	A-1,2	26	13.72	4-Butyrolactone	0.9	0.7	A-4
8	10.15	2-Methyl-2-pentene-1-one	1.0	3.9	A-2	27	13.99	Di(3-methylbutyl)amine	0.3	2.9	A-7
9	10.28	1-Hydroxy-2-butanone	2.0	8.2	A-1,2	28	15.93	Cyclooctane	2.2	0.1	A
10	10.38	Tetradecane	0.4	0.2	A	29	16.28	Guaiacol	1.3	0.5	C-5,8
11	10.52	Tetrahydro-6-methyl-2H-pyran-2-one	0	1.1	A-4	30	17.13	2-Ethylhexanoic acid	2.3	0.5	A-3
12	10.76	4-Hydroxy-3-hexanone	0.1	0.6	A-1,2	31	17.80	Phenol	9.6	4.5	C-8
13	11.00	2-Pentyl methoxyacetate	0.2	2.7	A-4,5	32	19.52	2-Hydroxy-4-butyrolactone	1.8	0	A-1,4
14	11.10	4-Heptanol	0.4	3.2	A-1	33	20.26	Syringol	1.9	0.7	C-5,8
15	11.25	1-Hydroxy-2-pentanone	0.8	3.9	A-1,2	34	20.85	4-Oxopentanoic acid	1.0	0.2	A-2,3
16	11.41	Acetic acid	19.3	5.2	A-3	35	21.67	3-Pyridinol	1.4	0	C-7,8
17	11.54	Furfural	5.4	0	B-6	36	22.36	5-Hydroxymethyl-2-furaldehyde	1.1	0	B-1,6
18	11.96	5-Hydroxy-4-octanone	0.3	0.3	A-1,2						
19	12.06	2,5-Hexanedione	0.8	0.3	A-2	Total			80.2	90.5	

[a]A = aliphatic, B = furan, C = aromatic, 1 = alcohol, 2 = ketone, 3 = carboxylic acid, 4 = ester, 5 = ether, 6 = aldehyde, 7 = amine, and 8 = phenol.

Table 4. Yields of Carbon Products Obtained from the Hydrothermal Treatment of Model Substrates in EFB Degradation[a]

Substrate	Additive	Product yield (%C) WS	WS HA[b]	WS HB[c]	WI	Gas	SR	Carbon balance (%)
Cellulose	Fe	93	27	7	2	6	2	103
Cellulose	none	58	2		23	7	8	96
Xylan	Fe	80	19	3	4	7	3	94
Xylan	none	64	2	1	18	5	7	94
Glucose	Fe	74	22	3	8	9	4	95
Glucose	none	53	5	3	26	6	10	95
Xylose	Fe	80	20	3	5	8	4	97
Xylose	none	64	2	1	19	5	6	94
Dihydroxyacetone	Fe	72	21		18	8	5	103
Dihydroxyacetone	none	41	2		31	8	17	97
Pyruvaldehyde	Fe	61	24		20	5	4	90
Pyruvaldehyde	none	35	2		27	6	17	85
Hydroxyacetone	Fe	96	81			3		99
Hydroxyacetone	none	95	103			3		98

[a]Reaction conditions: Substrate = 1 g, H_2O = 40 g, Fe = 1.564 g, P_{N2} = 1.0 MPa, temperature = 300 °C, and time =10 min. [b]Hydroxyacetone. [c]3-Hydroxy-2-butanone.

oligomers, which did not vaporize in the GC inlet. With the addition of Fe, the WS fraction contained significantly higher quantities of hydroxyketones than that obtained without Fe, which was in agreement with the NMR results (Figure 3), indicating that the addition of Fe increased the formation of aliphatic and oxygenated products. Previously, our group has reported that hydroxyacetone and 3-hydroxy-2-butanone are produced by the hydrogenation of degradation products from cellulose (Scheme S1), and the presence of Fe_3O_4 and/or dissolved Fe promotes the isomerization and retro-aldol condensation of sugars.[26] The aforementioned result indicates that the iron species in this novel system possibly functions as a catalyst for generating such precursors in the WS fraction. In addition, as shown in Table 2, a significantly higher yield of hydroxyketones was observed for the H_2O/EFB/Fe system, compared to the H_2O/EFB and H_2O/EFB/Oxidized Fe systems with or without added hydrogen. Furthermore, in the H_2O/EFB/Fe system, comparable yields of hydroxyketones were observed in the presence and absence of hydrogen, suggesting that highly active hydrogen is generated in situ and contributes to the formation of hydroxyketone components in the WS fraction.

Reactivities of Degradation Products. For examining the degradation characteristics and hydrothermal stability of the

DOI: 10.1021/acssuschemeng.7b00381
ACS Sustainable Chem. Eng. 2017, 5, 3562−3569

degradation products of EFB, possible intermediate compounds were tested under hydrothermal conditions, as summarized in Table 4. When saccharides such as cellulose, xylan, glucose, and xylose were used as substrates, the yield of the WS fraction was improved by the addition of Fe. Dihydroxyacetone and pyruvaldehyde, which are intermediates in the degradation of saccharides,[27] furnished similar results despite the fact that these aldehydes are known to form water-insoluble long chain molecules via aldol condensation under hydrothermal conditions. On the other hand, all substrates formed significant amounts of hydroxyacetone in the presence of Fe. Hydroxyacetone exhibited high hydrothermal stability both in the presence and absence of Fe. Thus, unstable aldehydes generated by the degradation of EFB are apparently converted into stable compounds such as hydroxyketones in the Fe/H_2O system, contributing to the high WS yield.

Based on these results, the positive effects of the H_2O/EFB/Fe system on the steam and hydrothermal liquefaction of EFB were investigated. In this system, Fe_3O_4 and active hydrogen were produced from the reaction between Fe and H_2O in both the steam and hydrothermal systems. Fe_3O_4 catalyzed the retro-aldol reaction of sugars under hydrothermal conditions, while the active hydrogen efficiently converted the highly reactive products into stable compounds. The stable compounds could not undergo successive condensation, cyclization, repolymerization, and carbonization, thus reducing char formation.

Regeneration and Reuse of Fe. Iron oxide can be reduced to metallic iron using biomass char[28] or biomass waste, such as sugar pine sawdust,[29] rice husk,[30] and palm kernel shells.[31] Because biomass wastes are renewable resources and CO_2 neutral, they are not only cost-effective but also eco-friendly as a reductant source. We recycled the oxidized Fe by using char and biomass. Figure 4 shows the XRD patterns of

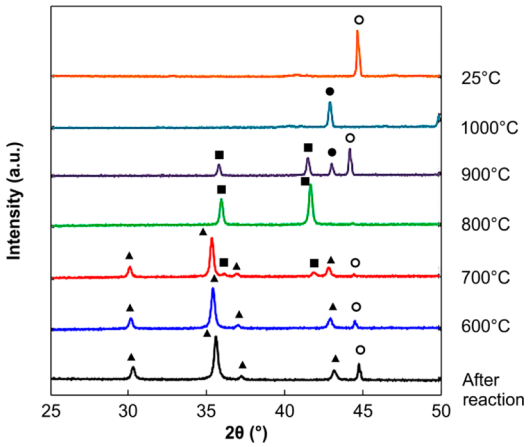

Figure 4. XRD patterns of the EFB/SR mixture containing oxidized Fe and heated at 600−1000 °C. (○) α-Fe, (●) γ-Fe, (▲) Fe_3O_4, and (■) FeO.

the EFB/SR mixture obtained at different temperatures. Signals observed at 30.2°, 35.5°, 37.2°, and 43.1° were attributed to Fe_3O_4 (Joint Committee on Powder Diffraction Standards (JCPDS) file No. 19-629), while a weak signal observed at 44.8° was attributed to α-Fe (JCPDS file No. 6-0696). By heating the mixture to 800 °C, Fe_3O_4 was transformed into FeO, and at 900 °C, the formation of Fe (43.0°, γ phase (JCPDS file No. 31-619) and 44.2°, α phase) was observed. At 1000 °C, only γ-Fe was present, which transformed into α-Fe upon cooling (C content < 0.1 wt %). These results confirmed that iron could be regenerated at 1000 °C in the presence of either EFB or char produced through the liquefaction of EFB as reductant.

For evaluating the reusability of Fe, the SR containing oxidized Fe and char was mixed with EFB and treated under N_2 at 1000 °C for 2 h. The hydrothermal liquefaction of EFB using regenerated Fe was conducted at a H_2O/EFB ratio of 40:1, and Table 5 summarizes the results. Compared to fresh Fe, using

Table 5. Reuse of Fe Regenerated from the Solid Residue Using EFB at 1000 °C[a]

	Carbon yield (%C)					
	WS					
Fe sample	WS	HA[b]	HB[c]	WI	Bio-oil	Gas
Fresh	69	20	7	15	84	5
Reuse #1	66	14	4	17	83	7
Reuse #2	64	14	5	9	73	8

[a]Reaction conditions: EFB = 1 g, H_2O = 40 g, P_{N2} = 1.0 MPa, temperature = 300 °C, time = 10 min. [b]Hydroxyacetone. [c]3-Hydroxy-2-butanone.

the regenerated Fe reduced the yield of bio-oil slightly from 84% to 73%, indicating that Fe is partly deactivated during regeneration. The increased peak intensities in the XRD patterns (Figure S3a) confirmed the presence of comparatively larger metal crystallites after regeneration. By field-emission transmission electron microscopy (FE-TEM), the average particle sizes of the fresh, used, and regenerated samples were 110, 85, and 548 nm, respectively, suggesting that Fe particles agglomerate during regeneration. In the first reuse cycle, the yields of hydroxyacetone and 3-hydroxy-2-butanone decreased (Table 5), but these yields were constant in the second cycle. This result indicated that the amount of generated hydrogen decreases with Fe regeneration. Therefore, it is possible that the decrease in bio-oil yields is attributed to increased char formation, which is due to the reduced amount of hydrogen generated from the reaction between aggregated Fe and H_2O.

Catalytic Cracking of the WS Fraction. The catalytic cracking of biomass pyrolysis vapors or bio-oil using solid acid catalysts could provide valuable hydrocarbons, which are currently obtained from fossil fuels (see Table S3).[15,32−34] Hence, the production of hydrocarbon from the WS fraction (40:1 H_2O/EFB) via catalytic cracking using HZSM-5 was evaluated (Table 6). The main gaseous products were observed in amounts with the following order: C_2−C_4 olefins > CO_2, CO > C_1−C_5 alkanes > BTX. Coke formation was not observed. Importantly, using WS obtained from the Fe-containing system, the yields of C_2−C_4 olefins and BTX were 1.9 times greater than those observed for the Fe-free system, although the formed amounts of CO_2, CO, and alkanes were comparable. The increase in the C_2−C_4 olefin yield is expected to be attributed to higher quantities of hydroxyketones in the WS fraction. Indeed, Huber and co-workers have reported that the yields of C_2−C_4 olefins and BTX from the catalytic cracking of water-soluble bio-oil increase after introducing an upgrading step of hydrogenation over Ru/C and Pt/C catalysts.[35]

Table 6 summarizes the results obtained from the catalytic cracking of the WS fraction using regenerated Fe. The total yields of C_2−C_4 olefins and BTX decreased over two reuse cycles. Therefore, the decrease in olefin yields is attributed to

DOI: 10.1021/acssuschemeng.7b00381
ACS Sustainable Chem. Eng. 2017, 5, 3562−3569

Table 6. Yields of Carbon Products Obtained from the Catalytic Cracking of the WS Fraction

	Carbon yield (%C)												
	Olefins				Alkanes				CO_x				
Production system of WS fraction	C_2	C_3	C_4	Sum	C_1	C_{2-5}	Sum	BTX	CO	CO_2	Sum	Water-solubles	Carbon balance (%)
H_2O/EFB	6	7	1	14	3	1	4	1	10	8	18	27	64
H_2O/EFB/Fe (fresh)	13	13	1	27	3	1	4	2	11	5	16	27	76
H_2O/EFB/Fe (reuse #1)	11	10	2	23	5		5	2	9	7	16	33	79
H_2O/EFB/Fe (reuse #2)	9	11	2	22	3	3	6	3	8	6	14	32	77

the decreased hydrogenated compound formation during the hydrothermal liquefaction of EFB.

As demonstrated by the experimental results discussed above, zerovalent Fe was successfully used for the hydrothermal liquefaction of EFB to produce bio-oil. This method, in which the hydrogen produced in the reaction was consumed to stabilize the degradation products of EFB, was more successful than the conventional H_2O/EFB approach. In addition, the used Fe was regenerated by heating it with SR and EFB at 1000 °C, although slightly lower product yields were obtained using the regenerated Fe. Our H_2O/EFB/Fe system was demonstrated to be suitable for the liquefaction of EFB to produce bio-oil, and it allows the control of the selectivity of the WS and WI components by varying the H_2O content. In addition, C_2–C_4 olefins were produced in good yields via the catalytic cracking of the WS fraction using the HZSM-5 zeolite catalyst. Nevertheless, additional studies must be conducted to further develop this system to transform biomass into valuable resources. Potential areas of study include the identification of the most efficient iron species for hydrogen generation, improvement of the hydrogen utilization efficiency, regeneration method for the oxidized Fe, and possible extension of this system to other biomass resources (e.g., other lignocellulosic biomass, algae, food waste, and sewage sludge). We postulate that the Fe/H_2O system developed herein can pave the route toward better utilization of biomass resources.

■ ASSOCIATED CONTENT

Supporting Information

The Supporting Information is available free of charge on the ACS Publications website at DOI: 10.1021/acssuschemeng.7b00381.

Composition of EFB, utilization rate of H_2, current and literature yields for light olefins obtained from biomass and related compounds, the continuous flow reactor used for catalytic cracking, GC–MS chromatogram chart of WS, XRD patterns, and FE-TEM images of the Fe samples, and a previously reported cellulose breakdown pathway (PDF)

■ AUTHOR INFORMATION

Corresponding Author

*Y. Kita. Tel.: +81-78-803-6244, Fax: +81-78–803-6512; E-mail: yuichi_kita@lion.kobe-u.ac.jp.

Author Contributions

All authors have equally contributed to this manuscript. All authors have given approval to the final version of the manuscript.

Notes

The authors declare no competing financial interest.

■ ACKNOWLEDGMENTS

The authors gratefully acknowledge financial support from Nippon Shokubai Co., Ltd. We would like to thank Editage (www.editage.jp) for English language editing.

■ ABBREVIATIONS

BTL, biomass-to-liquid
BTX, benzenes, toluene, and xylenes
EFB, empty fruit bunch
FE-TEM, field-emission transmission electron microscopy
GC–MS, gas chromatography–mass spectrometry
HT-XRD, high-temperature X-ray diffraction
SR, solid residue
WI, water-insoluble
WS, water-soluble

■ REFERENCES

(1) Ragauskas, A. J.; Williams, C. K.; Davison, B. H.; Britovsek, G.; Cairney, J.; Eckert, C. A.; Frederick, W. J.; Hallett, J. P.; Leak, D. J.; Liotta, C. L.; Mielenz, J. R.; Murphy, R.; Templer, R.; Tschaplinski, T. The path forward for biofuels and biomaterials. *Science* **2006**, *311* (5760), 484–489.

(2) Huber, G. W.; Iborra, S.; Corma, A. Synthesis of transportation fuels from biomass: Chemistry, catalysts, and engineering. *Chem. Rev.* **2006**, *106* (9), 4044–4098.

(3) Corma, A.; Iborra, S.; Velty, A. Chemical routes for the transformation of biomass into chemicals. *Chem. Rev.* **2007**, *107* (6), 2411–2502.

(4) Swain, P. K.; Das, L. M.; Naik, S. N. Biomass to liquid: A prospective challenge to research and development in 21st century. *Renewable Sustainable Energy Rev.* **2011**, *15* (9), 4917–4933.

(5) Kan, T.; Strezov, V.; Evans, T. J. Lignocellulosic biomass pyrolysis: A review of product properties and effects of pyrolysis parameters. *Renewable Sustainable Energy Rev.* **2016**, *57*, 1126–1140.

(6) Collard, F.-X.; Blin, J. A review on pyrolysis of biomass constituents: Mechanisms and composition of the products obtained from the conversion of cellulose, hemicelluloses and lignin. *Renewable Sustainable Energy Rev.* **2014**, *38*, 594–608.

(7) Tekin, K.; Karagöz, S.; Bektaş, S. A review of hydrothermal biomass processing. *Renewable Sustainable Energy Rev.* **2014**, *40*, 673–687.

(8) Akhtar, J.; Amin, N. A. S. A review on process conditions for optimum bio-oil yield in hydrothermal liquefaction of biomass. *Renewable Sustainable Energy Rev.* **2011**, *15* (3), 1615–1624.

(9) Arturi, K. R.; Kucheryavskiy, S.; Søgaard, E. G. Performance of hydrothermal liquefaction (HTL) of biomass by multivariate data analysis. *Fuel Process. Technol.* **2016**, *150*, 94–103.

(10) Bi, Z.; Zhang, J.; Peterson, E.; Zhu, Z.; Xia, C.; Liang, Y.; Wiltowski, T. Biocrude from pretreated sorghum bagasse through catalytic hydrothermal liquefaction. *Fuel* **2017**, *188*, 112–120.

(11) Nazari, L.; Yuan, Z.; Souzanchi, S.; Ray, M. B.; Xu, C. Hydrothermal liquefaction of woody biomass in hot-compressed water: Catalyst screening and comprehensive characterization of bio-crude oils. *Fuel* **2015**, *162*, 74–83.

DOI: 10.1021/acssuschemeng.7b00381
ACS Sustainable Chem. Eng. 2017, 5, 3562–3569

(12) Li, H.; Yuan, X.; Zeng, G.; Tong, J.; Yan, Y.; Cao, H.; Wang, L.; Cheng, M.; Zhang, J.; Yang, D. Liquefaction of rice straw in sub- and supercritical 1,4-dioxane−water mixture. *Fuel Process. Technol.* **2009**, *90* (5), 657−663.
(13) Zacher, A. H.; Olarte, M. V.; Santosa, D. M.; Elliott, D. C.; Jones, S. B. A review and perspective of recent bio-oil hydrotreating research. *Green Chem.* **2014**, *16* (2), 491−515.
(14) Patil, P. T.; Armbruster, U.; Martin, A. Hydrothermal liquefaction of wheat straw in hot compressed water and subcritical water−alcohol mixtures. *J. Supercrit. Fluids* **2014**, *93*, 121−129.
(15) Vispute, T. P.; Zhang, H.; Sanna, A.; Xiao, R.; Huber, G. W. Renewable chemical commodity feedstocks from integrated catalytic processing of pyrolysis oils. *Science* **2010**, *330* (6008), 1222−1227.
(16) Heo, E.; Kim, J.; Cho, S. Selecting hydrogen production methods using fuzzy analytic hierarchy process with opportunities, costs, and risks. *Int. J. Hydrogen Energy* **2012**, *37* (23), 17655−17662.
(17) Huisman, G. H.; Van Rens, G. L. M. A.; De Lathouder, H.; Cornelissen, R. L. Cost estimation of biomass-to-fuel plants producing methanol, dimethylether or hydrogen. *Biomass Bioenergy* **2011**, *35*, S155−S166.
(18) Kamarudin, S. K.; Daud, W. R. W.; Yaakub, Z.; Misron, Z.; Anuar, W.; Yusuf, N. N. A. N. Synthesis and optimization of future hydrogen energy infrastructure planning in peninsular Malaysia. *Int. J. Hydrogen Energy* **2009**, *34* (5), 2077−2088.
(19) Mueller-Langer, F.; Tzimas, E.; Kaltschmitt, M.; Peteves, S. Techno-economic assessment of hydrogen production processes for the hydrogen economy for the short and medium term. *Int. J. Hydrogen Energy* **2007**, *32* (16), 3797−3810.
(20) Olateju, B.; Kumar, A. Hydrogen production from wind energy in Western Canada for upgrading bitumen from oil sands. *Energy* **2011**, *36* (11), 6326−6339.
(21) Shibata, M.; Varman, M.; Tono, Y.; Miyafuji, H.; Saka, S. Characterization in chemical composition of the oil palm (Elaeis Guineensis). *J. Japan Inst. Energy* **2008**, *87* (5), 383−388.
(22) Sun, P.; Heng, M.; Sun, S.-H.; Chen, J. Analysis of liquid and solid products from liquefaction of paulownia in hot-compressed water. *Energy Convers. Manage.* **2011**, *52* (2), 924−933.
(23) Mullen, C. A.; Strahan, G. D.; Boateng, A. A. Characterization of various fast-pyrolysis bio-oils by NMR spectroscopy. *Energy Fuels* **2009**, *23* (5), 2707−2718.
(24) Kawamoto, H.; Hatanaka, W.; Saka, S. Thermochemical conversion of cellulose in polar solvent (sulfolane) into levoglucosan and other low molecular-weight substances. *J. Anal. Appl. Pyrolysis* **2003**, *70* (2), 303−313.
(25) Singh, R.; Balagurumurthy, B.; Prakash, A.; Bhaskar, T. Catalytic hydrothermal liquefaction of water hyacinth. *Bioresour. Technol.* **2015**, *178*, 157−165.
(26) Hirano, Y.; Kasai, Y.; Sagata, K.; Kita, Y. Unique approach for transforming glucose to C3 platform chemicals using metallic iron and a Pd/C catalyst in water. *Bull. Chem. Soc. Jpn.* **2016**, *89* (9), 1026−1033.
(27) Kabyemela, B. M.; Adschiri, T.; Malaluan, R. M.; Arai, K. Glucose and fructose decomposition in subcritical and supercritical water: Detailed reaction pathway, mechanisms, and kinetics. *Ind. Eng. Chem. Res.* **1999**, *38*, 2888−2895.
(28) Tang, H.; Qi, T.; Qin, Y. Production of low-phosphorus molten iron from high-phosphorus oolitic hematite using biomass char. *JOM* **2015**, *67* (9), 1956−1965.
(29) Strezov, V. Iron ore reduction using sawdust: Experimental analysis and kinetic modelling. *Renewable Energy* **2006**, *31* (12), 1892−1905.
(30) Purwanto, H.; Selamat, N. F. M.; Anto, P.; Akiyama, T. Pre-Reduced iron produced from low grade ore using biomass. *SEAISI Q. J.* **2010**, *39* (2), 18−22.
(31) Rashid, R. Z. A.; Salleh, H. M.; Ani, M. H.; Yunus, N. A.; Akiyama, T.; Purwanto, H. Reduction of low grade iron ore pellet using palm kernel shell. *Renewable Energy* **2014**, *63*, 617−623.
(32) Chen, N. Y.; Degnan, T. F. J.; Koenig, L. R. Liquid fuel from carbohydrates. *CHEMTECH* **1986**, *16* (8), 506−511.
(33) Adjaye, J. D.; Bakhshi, N. N. Production of hydrocarbons by catalytic upgrading of a fast pyrolysis bio-oil. Part I: Conversion over various catalysts. *Fuel Process. Technol.* **1995**, *45* (3), 161−183.
(34) Rezaei, P. S.; Shafaghat, H.; Daud, W. M. A. W. Production of green aromatics and olefins by catalytic cracking of oxygenate compounds derived from biomass pyrolysis: A review. *Appl. Catal., A* **2014**, *469*, 490−511.
(35) Zhang, H.; Cheng, Y.-T.; Vispute, T. P.; Xiao, R.; Huber, G. W. Catalytic conversion of biomass-derived feedstocks into olefins and aromatics with ZSM-5: The hydrogen to carbon effective ratio. *Energy Environ. Sci.* **2011**, *4*, 2297.

DOI: 10.1021/acssuschemeng.7b00381
ACS Sustainable Chem. Eng. 2017, 5, 3562−3569

Supporting Information

Fe-assisted hydrothermal liquefaction of lignocellulosic biomass for producing high-grade bio-oil

Yoshinori Miyata,[a] Kunimasa Sagata,[b] Mina Hirose,[b] Yoshiko Yamazaki,[b] Aki Nishimura,[a] Norimasa Okuda,[a] Yoshitaka Arita,[a] Yoshiaki Hirano,[b] and Yuichi Kita[b]*

[a]Strategic Technology Research Center, Nippon Shokubai Co., Ltd., Suita, Osaka 564-8512, Japan
[b]Department of Chemical Science and Engineering, Graduate School of Engineering, Kobe University, Kobe 657-8501, Japan

* Corresponding author
Yuichi Kita, E-mail: yuichi_kita@lion.kobe-u.ac.jp

Number of pages = 9
Number of tables = 3
Number of figures = 3
Number of schemes = 1

Table S1. Composition of oil palm empty fruit bunch (EFB)

Composition[1] (wt%)			Composition (wt%)		Composition[2] (wt%)			
Cellulose	Hemicellulose	Lignin	Moisture	Ash	C	H	N	O[3]
37.9	35.0	24.0	6.7	4.6	46.5	5.6	0.7	42.6

[1] See reference 1. [2] Percent weight on dry basis. [3] Calculated by difference.

Table S2. Production and consumption of H_2 from the reaction between Fe and H_2O at 300 °C

H_2O content (mL)	H_2 in the reactor (mmol) without EFB[a]	with EFB[b]	Utilization rate of H_2 (%)
1	13	9	31
3	24	9	63
5	25	10	60
10	22	13	41
40	20	13	35

Reaction conditions: [a] H_2O = 1–40 g, Fe = 1.564 g, P_{N2} = 1.0 MPa, temperature = 300 °C, time = 10 min. [b] EFB = 1 g, H_2O = 1–40 g, Fe = 1.564 g, P_{N2} = 1.0 MPa, temperature = 300 °C, time = 10 min.

Table S3. Yields of light olefins obtained via the catalytic cracking of biomass, biomass pyrolysis vapors, bio-oil, and bio-oil model compounds

Entry	Catalyst (Si/Al ratio)	Feed	Reactor	T (°C)	Feed/Cat. ratio (Feeding rate)	Olefin yield	Ref
1	HZSM-5 (24:1)	WS without Fe (C = 7299 ppm)	Fixed bed	600	1.1 g feed/g cat./h	14%-C	This study
2	HZSM-5 (24:1)	WS with Fe (C = 5584 ppm)	Fixed bed	600	1.1 g feed/g cat./h	27%-C	This study
3	HZSM-5 (24:1)	Tetrahydrofuran (12.5 wt%, C = 78690 ppm)	Fixed bed	600	9.7 g feed/g cat./h	46%-C	This study
4	HZSM-5 (24:1)	Tetrahydrofuran (2.9 wt%, C = 15441 ppm)	Fixed bed	600	1.3 g feed/g cat./h	44%-C	This study
5	HZSM-5 (24:1)	Tetrahydrofuran (12.5 wt%)	Fixed bed	600	11.7 g feed/g cat./h	51%-C	[2]
6	HZSM-5 (30:1)	WSBO[1] (12.5 wt%)	Fixed bed	600	11.7 g feed/g cat./h	19%-C	[2]
7	HZSM-5 (30:1)	WSBO[1] hydrogenation over Ru/C	Fixed bed	600	11.7 g feed/g cat./h	33%-C	[2]
8	HZSM-5 (30:1)	WSBO[1] hydrogenation over Ru/C and Pt/C	Fixed bed	600	11.7 g feed/g cat./h	51%-C	[2]
9	HZSM-5 (30:1)	40 wt% pine sawdust bio-oil, 60 wt% methanol	Fluidized bed	500	2.7 g feed/g cat./h	22 wt%	[3]
12	ZSM-5	Pine wood	Fluidized bed	600	0.35 g feed/g cat./h	9%	[4]
13	LOSA-1 and 10% Al_2O_3	Rice stalk	Fluidized bed	550	44 g/h	11%	[5]
14	ZSM-5	Rice stalk	Fluidized bed	550	44 g/h	11%	[6]

[1]WSBO = Water-soluble fraction of pinewood bio-oil.

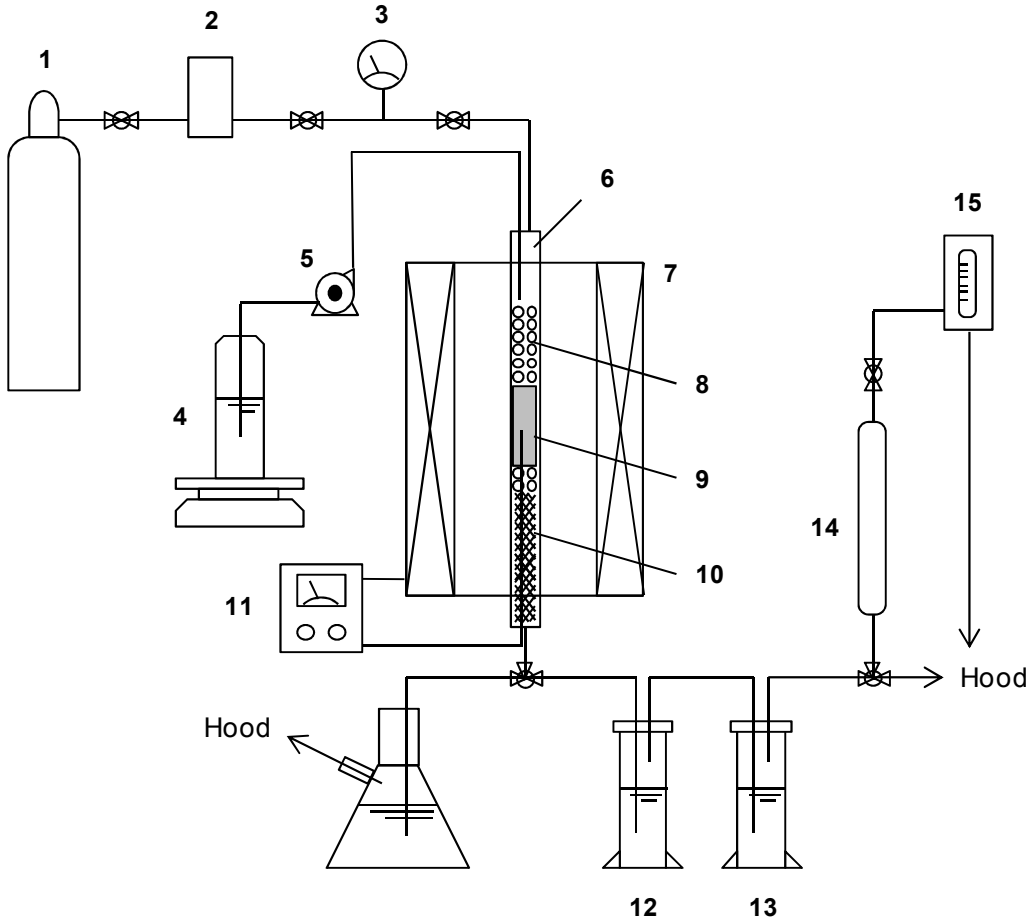

Figure S1. The fixed-bed continuous flow reactor for catalytically cracking the WS fraction into olefin and aromatics. **1**: N_2 gas cylinder, **2**: flow control, **3**: pressure gauge, **4**: aqueous solution of WS fraction, **5**: plunger pump, **6**: stainless steel tube reactor, **7**: tubular furnace, **8**: stainless steel beads, **9**: catalyst, **10**: stainless steel mesh, **11**: temperature control, **12**, **13**: gas wash bottles with water or acetone, **14**: gas sampling bottle, and **15**: soap film flowmeter.

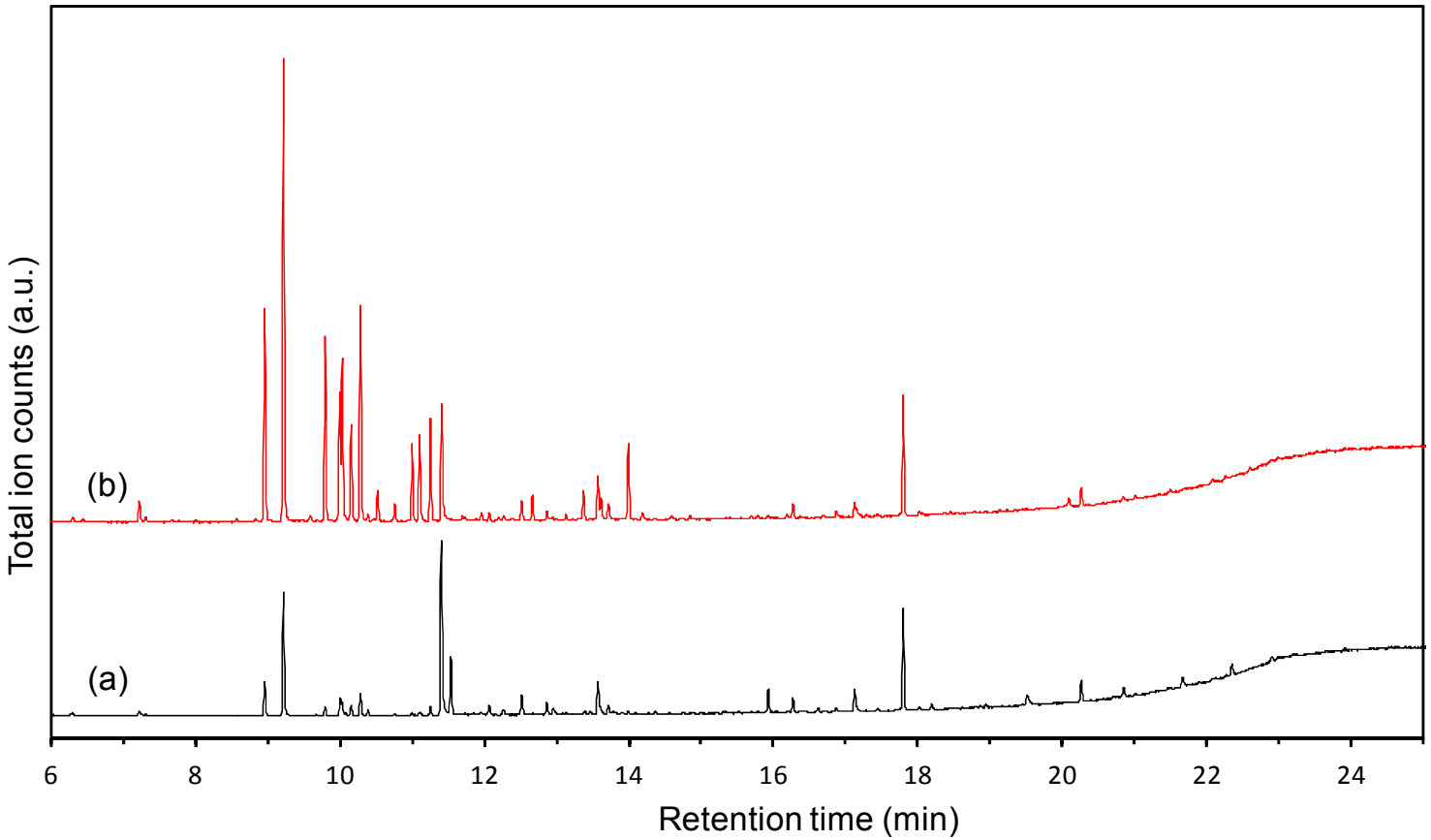

Figure S2. GC/MS spectra of the WS fraction obtained by the liquefaction of EFB at a H_2O/EFB weight ratio of 40:1 in the (a) absence and (b) presence of Fe.

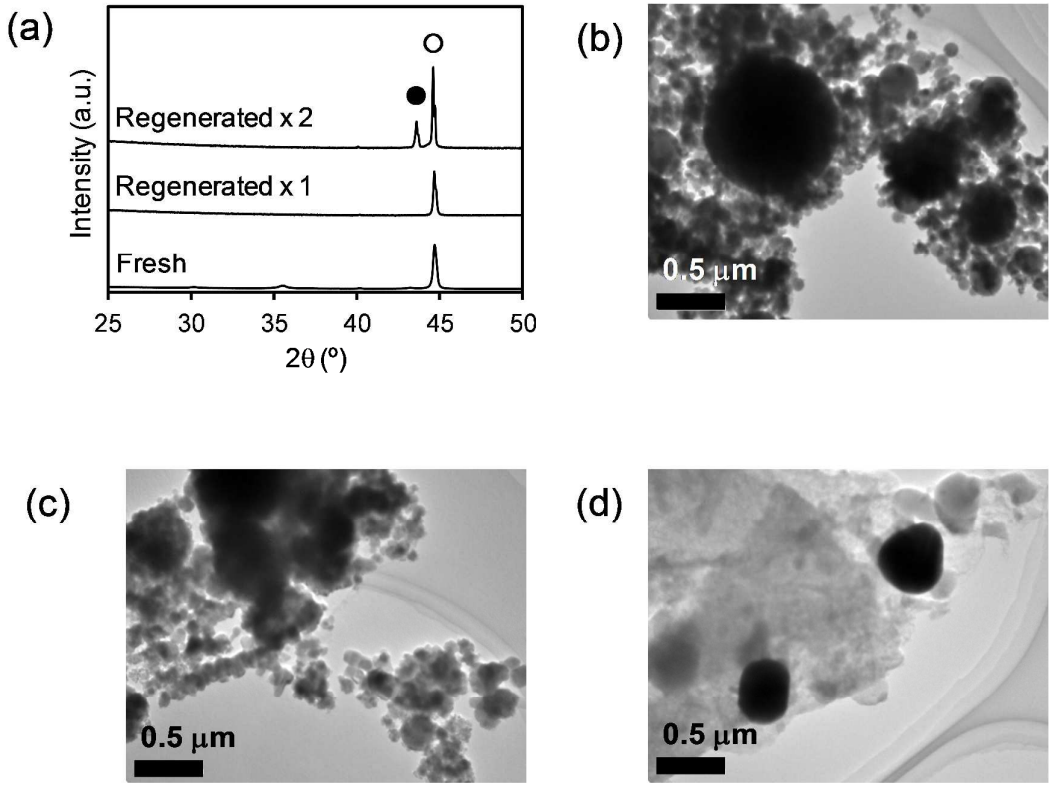

Figure S3. (a) XRD patterns ((○) α-Fe, (●) γ-Fe), and (b–d) FE-TEM images of the fresh, spent, and regenerated Fe samples, respectively.

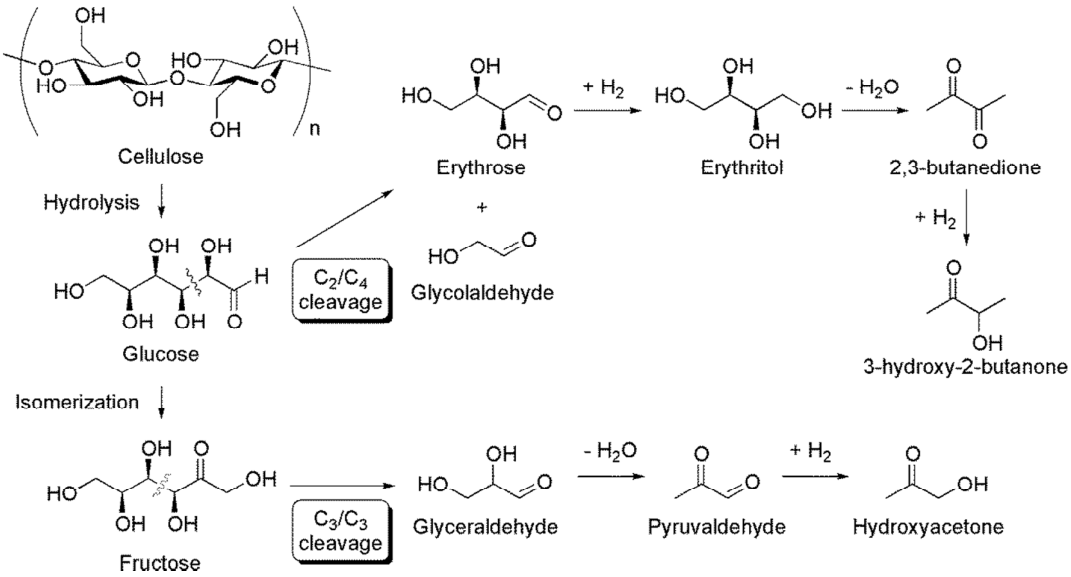

Scheme S1. Reaction pathway for the formation of hydroxyacetone and 3-hydroxy-2-butanone from cellulose.[7,8]

References

(1) Shibata, M.; Varman, M.; Tono, Y.; Miyafuji, H.; Saka, S. Characterization in chemical composition of the oil palm (Elaeis Guineensis). *J. Japan Inst. Energy* **2008**, *87* (5), 383–388.

(2) Zhang, H.; Cheng, Y.-T.; Vispute, T. P.; Xiao, R.; Huber, G. W. Catalytic conversion of biomass-derived feedstocks into olefins and aromatics with ZSM-5: the hydrogen to carbon effective ratio. *Energy Environ. Sci.* **2011**, *4*, 2297–2307.

(3) Valle, B.; Gayubo, A. G.; Alonso, A.; Aguayo, A. T.; Bilbao, J. Hydrothermally stable HZSM-5 zeolite catalysts for the transformation of crude bio-oil into hydrocarbons. *Appl. Catal. B.* **2010**, *100* (1), 318–327.

(4) Zhang, H.; Carlson, T. R.; Xiao, R.; Huber, G. W.; Huber, G. W.; Iborra, S.; Corma, A.; Kunkes, E. L.; Simonetti, D. A.; West, R. M.; et al. Catalytic fast pyrolysis of wood and alcohol mixtures in a fluidized bed reactor. *Green Chem.* **2012**, *14* (1), 98–110.

(5) Zhang, H.; Xiao, R.; Jin, B.; Xiao, G.; Chen, R. Biomass catalytic pyrolysis to produce olefins and aromatics with a physically mixed catalyst. *Bioresour. Technol.* **2013**, *140*, 256–262.

(6) Zhang, H.; Xiao, R.; Jin, B.; Shen, D.; Chen, R.; Xiao, G. Catalytic fast pyrolysis of straw biomass in an internally interconnected fluidized bed to produce aromatics and olefins: effect of different catalysts. *Bioresour. Technol.* **2013**, *137*, 82–87.

(7) Kabyemela, B. M.; Adschiri, T.; Malaluan, R. M.; Arai, K. Glucose and fructose decomposition in subcritical and supercritical water: detailed reaction pathway, mechanisms, and kinetics. *Ind. Eng. Chem. Res.* **1999**, *38*, 2888–2895.

(8) Yaylayan, V. A.; Keyhani, A. Origin of 2,3-pentanedione and 2,3-butanedione in d-glucose/ l-alanine Maillard model systems. *J. Agric. Food Chem.* **1999**, *47* (8), 3280–3284.